Engineering Structures 31 (2009) 2236–2246

Contents lists available at ScienceDirect

Engineering Structures

journal homepage: www.elsevier.com/locate/engstruct

Simulation of offshore wind turbine response for long-term extreme load prediction

Puneet Agarwal [1], Lance Manuel *

Department of Civil, Architectural, and Environmental Engineering, University of Texas at Austin, Austin, TX 78712, USA

ARTICLE INFO

Article history:
Received 9 July 2007
Received in revised form
4 April 2009
Accepted 6 April 2009
Available online 8 May 2009

Keywords:
Offshore wind turbines
Long-term loads
Extrapolation
Inverse reliability
Control actions
Response variability

ABSTRACT

When there is interest in estimating long-term extreme loads for an offshore wind turbine using simulation, statistical extrapolation is the method of choice. While the method itself is rather well-established, simulation effort can be intractable if uncertainty in predicted extreme loads and efficiency in the selected extrapolation procedure are not specifically addressed. Our aim in this study is to address these questions in predicting blade and tower extreme loads based on stochastic response simulations of a 5 MW offshore turbine. We illustrate the use of the peak-over-threshold method to predict long-term extreme loads. To derive these long-term loads, we employ an efficient inverse reliability approach which is shown to predict reasonably accurate long-term loads when compared to the more expensive direct integration of conditional load distributions for different environmental (wind and wave) conditions. Fundamental to the inverse reliability approach is the issue of whether turbine response variability conditional on environmental conditions is modeled in detail or whether only gross conditional statistics of this conditional response are included. We derive long-term loads for both these cases, and demonstrate that careful inclusion of response variability not only greatly influences such long-term load predictions but it also identifies different environmental conditions that bring about these long-term loads compared with when response variability is only approximately modeled. As we shall see, for this turbine, a major source of response variability for both the blade and tower arises from blade pitch control actions due to which a large number of simulations are required to obtain stable distribution tails for the turbine loads studied.

1. Introduction

Statistical extrapolation of extreme loads is being increasingly used in the design of offshore wind turbines against ultimate limit states, and a recent draft [1] of design guidelines from the International Electrotechnical Commission (IEC) also recommends its use. Statistical extrapolation involves integration of the distribution of turbine loads given specified environmental states with the likelihood of occurrence of the different environmental states; the (conditional) load distributions are obtained by means of turbine response simulations.

While extrapolation methods are relatively well understood for onshore wind turbines [e.g., [2–4]], they present several challenges for offshore turbines. For one, the offshore environment involves, as a minimum, the consideration of waves in addition to wind; hence, the number of random variables describing the environment increases. As a result, the domain of integration expands and it can often become impractical to perform computationally expensive simulations over this entire domain if one uses the basic extrapolation approach that involves direct integration. It is thus of interest to explore efficient alternative extrapolation techniques for offshore wind turbine design. A second challenge is that extrapolation of turbine loads needs to recognize the dependence on two (or more) random processes representing the environment—wind and waves, say—each of which influence turbine loads in distinct ways. Several studies in recent years have focused on the complexity of these issues in the offshore environment and have addressed comparisons of alternative methods to extract turbine load extremes [5], possible reduction in simulation effort by careful selection of critical environmental states [6], use of the environmental contour method [7], and use of a suitable percentile of the wave-related random variable (conditional on wind speed) in lieu of the full joint wind-wave distribution [8].

On related matters to those highlighted in these previous efforts, we attempt here to answer several open questions regarding how the peak-over-threshold method should be used with the environmental contour method; whether or not the environmental contour method, which requires considerably less simulation effort is as accurate as direct integration in statistical

* Corresponding author. Tel.: +1 512 232 5691; fax: +1 309 413 8986.
E-mail addresses: Puneet.Agarwal@stress.com (P. Agarwal), lmanuel@mail.utexas.edu (L. Manuel).

[1] Currently at Stress Engineering Services, Houston, TX, USA.

0141-0296/$ – see front matter © 2009 Elsevier Ltd. All rights reserved.
doi:10.1016/j.engstruct.2009.04.002

load extrapolation; and whether or not variability in turbine loads must be carefully accounted for in order to yield accurate long-term loads. To address these issues, we derive long-term loads using a model of a utility-scale 5MW offshore wind turbine that was developed at the National Renewable Energy Laboratory (NREL), and which is assumed to be sited in 20 m of water. Stochastic time-domain simulations of turbine response form the basis for this study. While the inflow turbulence describing the wind field is simulated using similar procedures to those for onshore turbines, excitation from waves is simulated assuming simplified linear irregular wave kinematics that may not be suitable for this shallow-water site. In shallow waters, irregular waves are more appropriately modeled using a second-order wave theory such as that developed by Sharma and Dean [9]. While such nonlinear wave modeling capabilities were not fully integrated with wind turbine aeroelastic simulation software such as FAST [10] at the time of this writing, such enhancements are planned, given the preponderance of shallow-water sites for offshore wind turbines.

The outline of this work is as follows: after describing the extrapolation methods and the simulation model, we examine turbine response statistics for several representative environmental conditions. We then discuss application of the peak-over-threshold (POT) method to derive probability distributions of turbine loads. We illustrate how long-term loads can be derived using the Inverse First-Order Reliability Method, first by omitting turbine load variability as in the environmental contour (EC) method, and then by explicitly accounting for this variability (given environmental state). Comparison of EC-based long-term load predictions with those obtained by direct integration is discussed. We also discuss how turbine control actions influence variability in long-term loads. Finally, we compare predictions of rare (long-term) load fractiles based on the POT and global maxima methods.

2. Load extrapolation methods

Design Load Case (DLC) 1.1b of the IEC 61400-3 draft design guidelines [1] for offshore wind turbines, which is based on DLC 1.1 of the IEC 61400-1 guidelines [11] for onshore wind turbines, recommends the use of statistical extrapolation methods to predict turbine characteristic loads for an ultimate limit state. In direct integration, which is most often employed in statistical extrapolation for wind turbine extreme loads, one seeks to estimate the turbine long-term load, l_T, associated with an acceptable exceedance probability, P_T, or equivalently with a target service life of T years, using the following equation:

$$P_T = P[L > l_T] = \int_X P\left[L > l_T | X = x\right] f_X(x)\mathrm{d}x \tag{1}$$

where $f_X(\boldsymbol{x})$ is the joint probability density function of the environmental random variables, $\boldsymbol{X}$, and L is the random variable describing the load of interest. For different trial values of load, l_T, Eq. (1) enables one to compute the long-term probability of exceeding that load by integrating the short-term load exceedance probability conditional on $\boldsymbol{X}$, i.e., $P\left[L > l_T | X = x\right]$, with the relative likelihood of different environmental conditions, $\boldsymbol{X}$. The load level at which the computed long-term probability matches the target probability is the desired characteristic T-year load. The direct integration method, while exact, is computationally expensive as one is required to integrate over the entire domain of all the environmental random variables. For offshore wind turbines, $\boldsymbol{X}$ is usually assumed to be comprised of the ten-minute mean wind speed, V, at hub height in the along-wind direction and the significant wave height, H_s (four times the standard deviation of the sea surface elevation process), for waves assumed to be aligned with the wind. The averaging duration of ten minutes is standard practice for wind turbines [1,11]. When such ten-minute time series are simulated to yield statistics on L, the T-year load, l_T, is expressed in terms of the distribution of L as follows:

$$\begin{aligned} P_T &= P(L > l_T) = 1/(T \times 365.25 \times 24 \times 6) \\ &= 1.90 \times 10^{-5}/T. \end{aligned} \tag{2}$$

It is convenient to define a target reliability index, β, that is associated with the target return period, T, and thus with P_T such that $\Phi(-\beta) = P_T$, where $\Phi()$ refers to the standard Gaussian cumulative distribution function.

The flowchart in Fig. 1 shows how turbine response simulations are used to establish the long-term load distribution using direct integration. For specific choices of the environmental random variable vector, $\boldsymbol{X} = \boldsymbol{x}$, we first seek to establish the short-term distribution of load conditional on the environment, $F_{L|X=x}(l)$. To do so, M load extremes, L_r $(r = 1, 2, \ldots M)$, are extracted from repeated simulations. These extremes can then be used to establish an empirical (short-term) distribution function, to which a parametric probability distribution model may be fit if desired. A global maximum, defined as the single largest maximum value obtained from a turbine response time series of ten-minute duration (the chosen duration here, as recommended by design standards [1,11]), is an example of a load extreme. Peak-over-threshold (POT) maxima represent another choice of extreme statistics that may be extracted from each ten-minute sample; POT extremes will be discussed later. To obtain a single time series realization of the stochastic turbine response process, we first simulate a ten-minute realization of the inflow stochastic 3-D wind velocity field on a gridded 2-D rotor plane; this is achieved using standard Fourier approaches together with target turbulence power spectra and coherence functions [11,12]. The incident sea surface elevation process at the location of the turbine support structure is also simulated, generally using a linear irregular (stochastic) wave modeling approach. Once these environmental inputs are in place, the response of the turbine is computed using an aero-servo-hydro-elastic analysis in the time domain. Due to the nature of the machine-specific airfoil data for blades, matching control systems, etc., the response computations are usually carried out using integrated simulation software such as FAST [10]. By varying a set of random seeds, s_r, that produces different realizations of the stochastic wind and wave processes for the same environmental conditions, $\boldsymbol{x}$, and thus generates a different realization of the turbine response each time, one can obtain the desired M load extremes. Once the short-term load distributions for all $\boldsymbol{X}$ (i.e., for all combinations of mean wind speed and significant wave height in our case) are established, we can integrate them with the joint probability distribution function of the environmental random variables, $f_X(\boldsymbol{x})$, in order to obtain the long-term load distribution using Eq. (1).

The direct integration method is computationally expensive as it requires multiple simulations over the entire domain of the environmental variables, $\boldsymbol{X}$. Therefore, it is of interest to explore more efficient methods for extrapolation—an inverse first-order reliability method (IFORM) [13] approach is one such alternative efficient procedure. To understand IFORM, it is instructive to first consider a sphere of radius equal to β, i.e., the reliability index, in a three-dimensional space, $\boldsymbol{U}$, describing independent standard normal variables, U_1, U_2, and U_3, one for each of the physical random variables (V, H_s, and L) in the problem of interest. On such a sphere, we have:

$$u_1^2 + u_2^2 + u_3^2 = \beta^2. \tag{3}$$

The probability of occurrence of values on the side of a tangent plane to the sphere away from the origin is computed as $\Phi(-\beta)$. In our case, the standard normal random variables, U_1, U_2, and

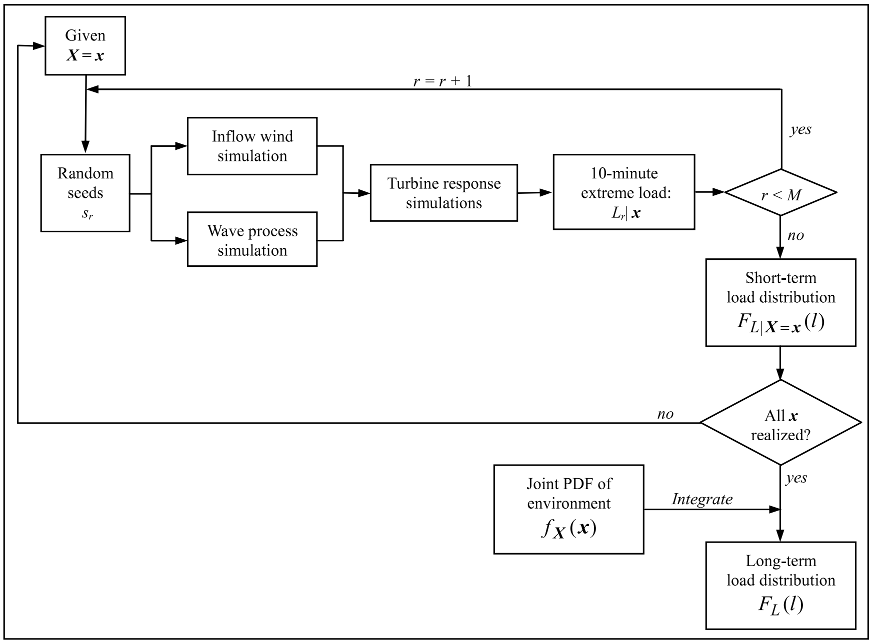

Fig. 1. Flowchart describing the steps involved in establishing short-term and long-term load distributions based on turbine response simulations. A total of M simulations are carried out for each realization, $\boldsymbol{x}$, of the environmental random variable vector, $\boldsymbol{X}$. For the rth single simulation (where r varies from 1 to M), the seeds, s_r, lead to a single 10-min extreme load, L_r. Once all M simulations are carried out, the short-term distribution, $F_{L|X=x}(l) = P[L < l|\boldsymbol{X} = \boldsymbol{x}]$ is established. By varying $\boldsymbol{x}$, the long-term distribution, $F_L(l)$ is established by weighting the short-term load distribution by the environmental variables' joint probability density function, $f_X(\boldsymbol{x})$.

U_3 are related to physical random variables, V, H_s, and L; thus, all points on the sphere can be thought to represent combinations of variables associated with equal probability. Since each point on the sphere is associated with the same reliability index, the desired load, l_T, is also associated with this same reliability—it represents the largest value that L can have among all possible values on the surface of the sphere. The only apparent complication is that the sphere is in a three-dimensional space of independent standard normal variables, not in the physical space of the jointly distributed variables, V, H_s, and L. If, however, a mapping (such as the Rosenblatt transformation [14]) were possible, again, since each point on the sphere is associated with the same (target) reliability, all of these points on the sphere need to be systematically searched until the largest load, L, is found. This largest load is then, by definition, l_T. This procedure is the inverse first-order reliability method (IFORM) [13].

A simplified version of the inverse first-order reliability method is the environmental contour (EC) method [13], which represents the response random variable, conditional on the environmental variables, only at its median value. Based on the Rosenblatt transformation, u_3 is thus identically zero. As such, the EC method does not utilize nor need the full distribution of the load given the environmental random variables (as established from simulations). Since $u_3 = 0$, the sphere of radius, β, reduces to a circle (such that $u_1^2 + u_2^2 = \beta^2$), whose transformation onto the physical space is termed an "environmental contour". Analogous to the 3-D case, one is now required to search for the point of maximum median load (i.e., the design point) by only considering those environmental states defined on this environmental contour. It can be easily shown that the environmental contour method essentially approximates the solution for l_T in Eq. (1) by replacing the conditional cumulative distribution of L given V and H_s by a step function, $H(f_L(V, H_s))$, where $f_L(V, H_s) = L_{med}(V, H_s) - l_T$, and $H(y) = 1$, if $y > 0$, and 0 otherwise; also $L_{med}(V, H_s)$ represents the "median" load given V and H_s. The reader is referred to other studies [3,7] for more details on the environmental contour method as applied to wind turbines.

3. Simulation model

A 5MW wind turbine model [15] developed at NREL and closely representing utility-scale offshore wind turbines being manufactured today is used in our simulation studies. The turbine is assumed to have a hub height of 90 m above the mean sea level, and a rotor diameter of 126 m. The turbine is a variable-speed and collective pitch-controlled machine, with a maximum rotor speed of 12.1 rpm. The rated wind speed is 11.5 m/s. The turbine is assumed to be sited in 20 m of water; it has a monopile support structure, which is assumed to be rigidly connected at the mudline. The turbine is assumed to be installed at an IEC Class I-B wind regime site [1,11]. A Kaimal power spectrum and an exponential coherence spectrum are employed to describe the turbulence random field over the rotor plane, which is simulated using the computer program, TurbSim [12]. For the hydrodynamic loading on the support structure, irregular linear long-crested waves are simulated using a JONSWAP spectrum [16]. Hydrodynamic loads are computed using Morison's equation; Wheeler stretching is used to account for the influence of the instantaneous sea surface elevation on kinematics and hydrodynamics. Once time histories of the wind velocity field and the sea surface elevation processes are generated, stochastic time-domain simulations of the turbine response are performed using a combined modal and multi-body dynamics formulation [10] that models the tower and blades as flexible bodies using their first two bending modes in the longitudinal and transverse directions. Nacelle yaw motion, generator speed, torsional flexibility of the drivetrain, etc. are all accounted for as well in the analysis, as needed.

4. Turbine response

We are interested in the response of the turbine only while it is in an operating state. Accordingly, we perform response simulations for mean wind speeds ranging from cut-in to cut-out wind speeds (i.e., 3 to 25 m/s, here). As a function of the mean wind speed in each simulation, the turbulence intensity is assumed per IEC Class I-B site conditions using the Normal Turbulence Model

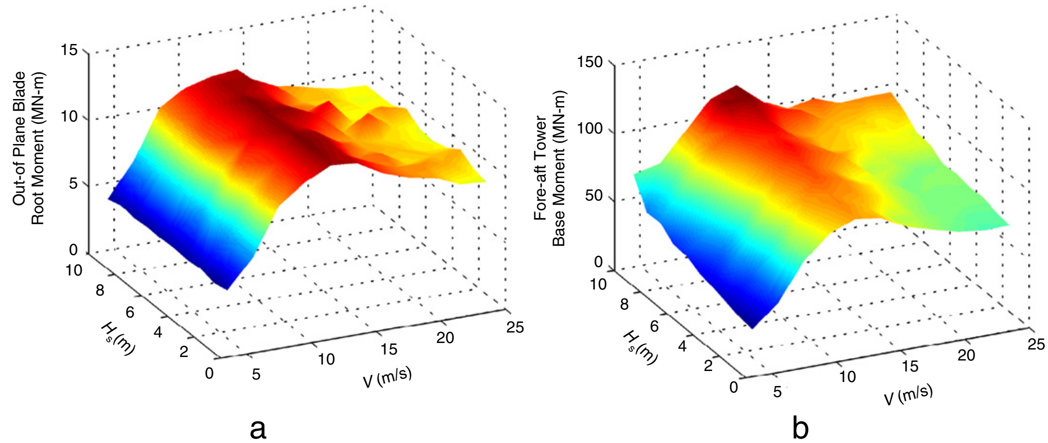

Fig. 2. Variation with mean wind speed and significant wave height of the mean of the maximum values from six simulations of (a) the out-of-plane blade root moment; and (b) the fore-aft tower base moment.

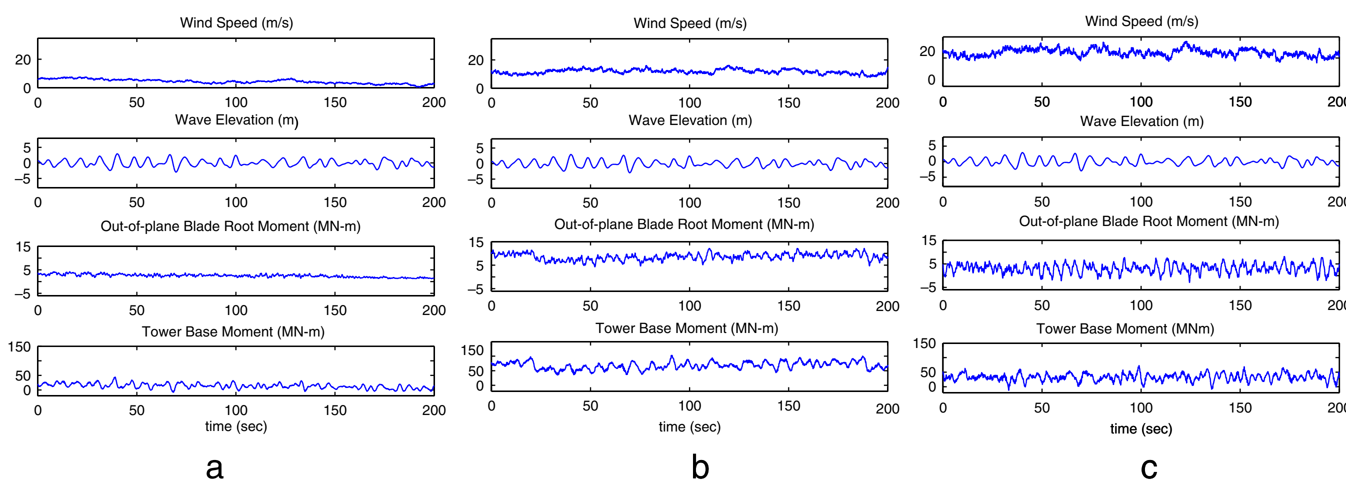

Fig. 3. Representative time series of wind speed, sea surface elevation, out-of-plane blade moment, and tower bending moment for mean wind speeds of (a) 3.7 m/s, (b) 12.1 m/s and (c) 24.2 m/s. The significant wave height is fixed at 4.2 m.

(NTM) [11]. The peak spectral period for the waves is modeled as a function of significant wave height based on one year's data from the National Oceanic and Atmospheric Administration's National Data Buoy Center's Buoy 44007, where the water depth is 19 m. We discretize the domain of the two environmental random variables using a two-dimensional interval or bin of 2 m/s for mean wind speed and 1 m for significant wave height. We will focus on the out-of-plane blade moment (OoPBM) at the blade root and the fore-aft tower base moment (TBM) at the mudline as the two turbine load variables whose extreme values are of interest in this study.

In order to derive statistics or distributions of turbine loads conditional on wind speed and wave height, multiple simulations have to be carried out for selected pairs of mean wind speed and significant wave height values. Fig. 2 shows the average of ten-minute maximum loads from six simulations for each V–H_s bin considered. It is observed that the maximum out-of-plane blade moment increases with wind speed, up to the rated wind speed of 11.5 m/s, and then decreases, as is expected due to blade-pitch control actions. Also blade loads are seen to be relatively insensitive to wave height. On the other hand, the maximum fore-aft tower base moment, while it also peaks at the rated wind speed, is seen to increase almost linearly with wave height.

To investigate the effect of wind on turbine loads in greater detail, we compare the turbine response for mean wind speeds of 3.7 m/s, 12.1 m/s, and 24.2 m/s, while the significant wave height is held constant at 4.2 m. Figs. 3 and 4 suggest that in general blade and tower loads have increased energy (variance) with increasing wind speed. Even though maximum blade moments are higher around the rated wind speed (see Figs. 3(b) and 2(a)), the variance is smaller there than at 24.2 m/s (Figs. 3(c) and 4(b)). Such response is due to blade pitch control actions which act to reduce aerodynamic forces on blades by limiting the rotor speed when the instantaneous wind speed increases above the rated wind speed (11.5 m/s, here). As a result, mean blade loads (as well as mean tower loads) reduce as the mean wind speed is increased from rated to cut-out. Additionally, though, in each ten-minute simulation, the instantaneous wind speed fluctuates about the mean wind speed (these fluctuations are described by the turbulence standard deviation which is directly proportional to the mean wind speed here); hence, with increasing wind speed, the blade pitch angle, the aerodynamic forces and, ultimately, blade loads show significant variability as is evidenced by their larger variance at the larger mean wind speeds.

Note that tower load variance differences between rated and very high wind speeds are smaller than is the case for blade loads. Important peaks in the power spectra of the loads are seen at the so-called 1P frequency (corresponding to the rotor rotation rate of 0.2 Hz at and above the rated wind speed) and at multiples of this frequency, where the peaks are dominant, as well as at resonant frequencies associated with edgewise and flapwise modes (both of which are present in the OoPBM process) and with tower fore-aft bending. These resonant frequencies were computed from a

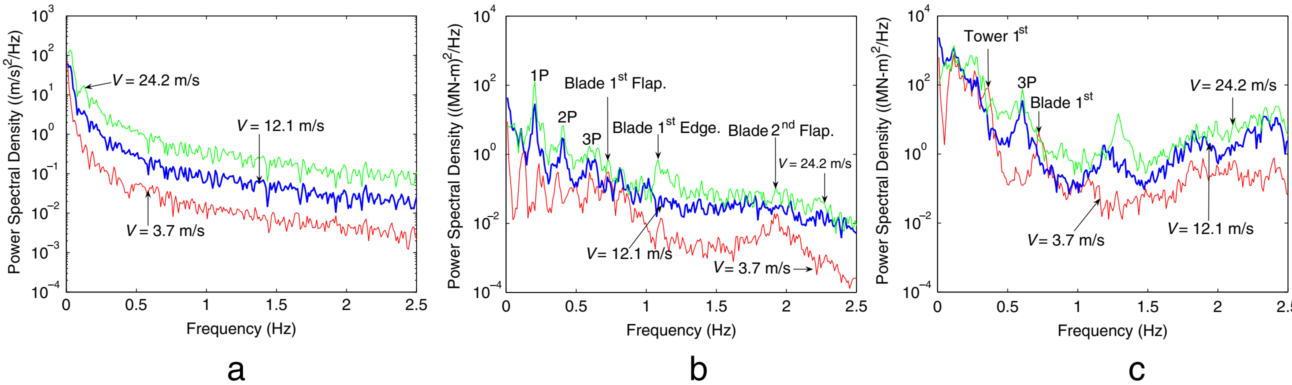

Fig. 4. Variation of power spectral density with mean wind speed for (a) wind speed, (b) out-of-plane blade moment, and (c) tower bending moment. The significant wave height is fixed at 4.2 m.

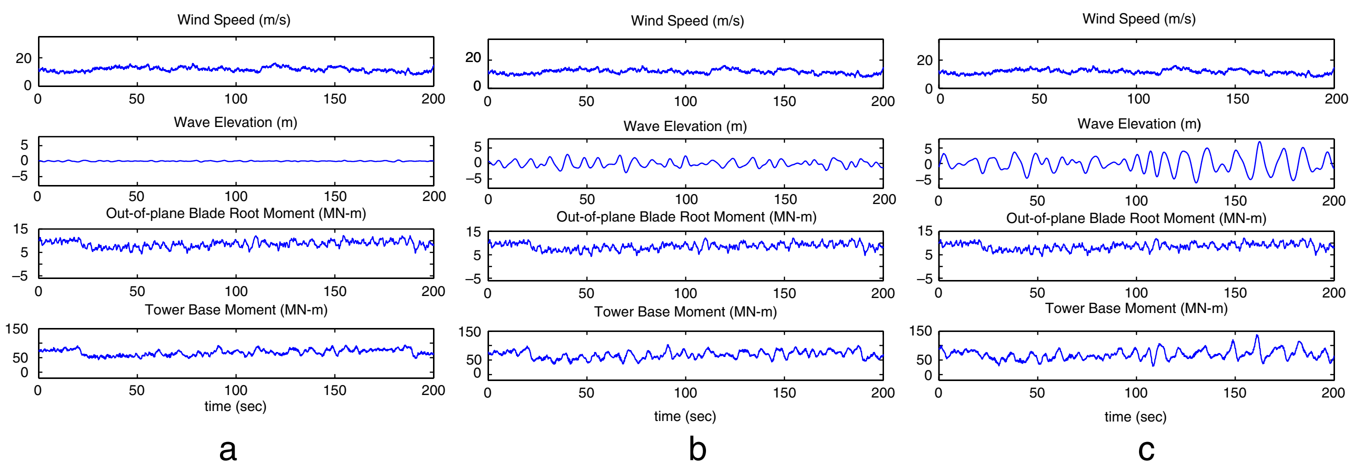

Fig. 5. Representative time series of wind speed, sea surface elevation, out-of-plane blade moment, and tower bending moment for significant wave heights of (a) 0.5 m, (b) 4.2 m and (c) 9.4 m. The mean wind speed is fixed at 12.1 m/s.

linearized modal analysis of the nonlinear aeroelastic model of the wind turbine [10].

The effect of waves is studied by comparing the turbine response for significant wave heights of 0.5 m, 4.2 m and 9.4 m, while the mean wind speed is held constant at 12.1 m/s. Fig. 5 clearly shows larger peaks in the TBM time series with increasing wave heights. Blade loads are seen to be insensitive to wave height variation. Accordingly, power spectra for tower loads alone are presented in Fig. 6 where no significant influence of wave height is noted, except at frequencies below around 0.2 Hz where wave energy is dominant, with sea surface elevation peak spectral frequencies occurring at 0.14, 0.10 and 0.08 Hz for significant wave heights of 0.5, 4.2 and 9.4 m, respectively.

Table 1 summarizes statistics of the blade and tower loads obtained from six simulations each for the wind and wave conditions discussed in Figs. 3–6. OoPBM statistics, as was discussed before, are insensitive to wave height. Also, the mean and maximum OoPBM are systematically higher around the rated wind speed compared to other wind speeds—e.g., the maximum OoPBM load near the rated wind speed is about 37% larger than it is near the cut-out wind speed. Table 1 also presents values of the skewness, kurtosis and peak factors of the turbine loads; these statistics provide some insights into the non-Gaussian character of the load processes. Assuming that a process is Gaussian, one can estimate a theoretical peak factor (which describes maxima in terms of the number of standard deviations above the mean) from knowledge of the number of maxima in each time series realization (here, of ten-minute duration) [17]. For the OoPBM process, a

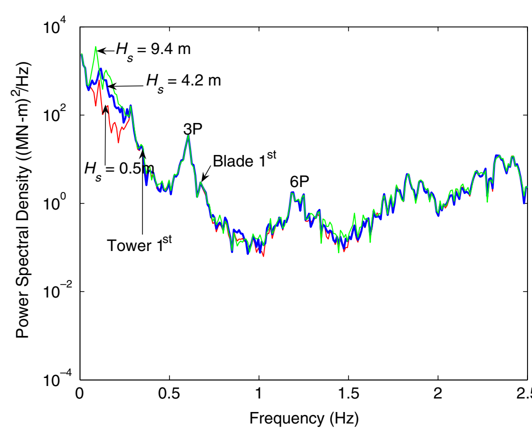

Fig. 6. Variation of power spectral density of fore-aft tower bending moment with significant wave height. The mean wind speed is fixed at 12.1 m/s.

Gaussian peak factor for all three wind speeds and wave heights is about 3.3, which is larger than the computed peak factors (shown in Table 1) when the skewness is negative, and smaller when the skewness is positive (only for the case where $V = 4$ m/s and $H_s = 4.5$ m). Note that kurtosis values for the OoPBM process are also somewhat different from those for a Gaussian process, whose kurtosis value is 3.0. The implication of the non-Gaussian character of the turbine load processes is that extremes associated with rare (low probability of exceedance) levels may be very different from

Table 1
Ten-minute statistics of turbine loads for different wind speed and wave height bins.

V (m/s)	H_s (m)	Out-of-plane moment at the blade root						Fore-aft tower base moment					
		Max (all in MN m)	Mean	SD	Skew. –	Kurt.	PF	Max (all in MN m)	Mean	SD	Skew. –	Kurt.	PF
12.0	0.5	12.5	8.2	1.5	−0.05	2.64	2.85	97.3	65.2	10.9	0.11	2.41	2.96
12.0	4.5	12.7	8.3	1.6	−0.25	2.74	2.80	106.6	66.3	12.7	−0.03	2.76	3.17
12.0	9.5	12.2	8.2	1.5	−0.14	2.61	2.60	124.2	66.2	16.1	0.18	3.08	3.61
4.0	4.5	4.5	2.3	0.6	0.49	2.83	3.65	39.4	12.3	8.6	0.07	2.79	3.16
12.0	4.5	12.7	8.3	1.6	−0.25	2.74	2.80	106.6	66.3	12.7	−0.03	2.76	3.17
24.0	4.5	9.3	3.0	2.0	−0.14	2.89	3.07	78.4	32.8	12.3	0.07	3.07	3.73

Note: V: Mean wind speed, H_s: Significant wave height, Max: Ten-minute maximum, SD: Standard deviation, Skew.: Skewness, Kurt.: Kurtosis, PF: Peak Factor = (Max − Mean)/SD.

those predicted by a Gaussian process with the same mean and variance.

The TBM process statistics are also interesting—when studied with variation in wave height, it is seen that mean levels change only very slightly. This is because the sea surface elevation process has a zero mean, and changes in significant wave height do not affect the mean response, especially since no current is assumed present. On the other hand, as the significant wave height is increased from 4.5 m to 9.5 m, the standard deviation and maximum values of the TBM increase by about 27% and 17%, respectively. This is because significant wave height, which is directly related to the energy (variance) of the wave process, directly affects the energy in the turbine response process; hence, the maximum and variance of the TBM process increase systematically with wave height. As was the case for the blade loads, peak factors for the TBM process are different from those for a Gaussian process, as are skewness and kurtosis values. Again, these reflect the non-Gaussian nature of the tower load process.

From the preceding results, it can be concluded that: (1) blade and tower loads are largest around the rated wind speed, but peak factors are lowest there; (2) blade loads are independent of wave height; and (3) maximum tower loads increase systematically with wave height. Hence, turbine long-term extreme loads are expected to be governed either by mean wind speeds near rated (for instance, the mean and maximum blade bending loads are higher there) or by higher-than-rated wind speeds where larger variability in loads and associated large peak factors could lead to large extreme values. Also, tower long-term extreme loads are likely to result from larger wave heights.

5. Short- and long-term loads

5.1. Short-term extreme load distributions

The short-term distribution of turbine extreme loads, $F_{L|X}(l)$, which enables prediction of long-term loads according to Eq. (1), requires data on load extremes. The global maximum and peak-over-threshold methods are commonly used to extract load extremes from time series data. We use the peak-over-threshold method here, as it can provide a large number of load extremes from a given number of simulations, resulting in better definition of distribution tails which is important when extrapolating loads to rare fractiles or low probability of exceedance levels.

In the peak-over-threshold (POT) method, the maximum load from each segment of a time series that lies between two successive upcrossings of a chosen threshold is retained as a load extreme. While the choice of threshold may be optimized [4], here we choose a threshold fixed at a mean plus 1.4 SD level [2], which is also suggested by the IEC standard [11]. The mean and standard deviation used are based on all the load time series simulations carried out for a wind speed and wave height bin ($\boldsymbol{X}$). The cumulative distribution function for load extremes, $F_{L|X=x}(l)$is:

$$F_{L|X=x}(l) = \left[F_{L_{POT}|X=x}(l)\right]^n \tag{4}$$

where n is the expected number of peaks (above the chosen threshold) in ten minutes, and $F_{L_{POT}|X=x}(l)$ represents the cumulative distribution function of POT-based load extremes. This distribution is established non-parametrically here since distribution tails from a limited number of simulations—six, here—are not stable enough to allow parametric model fits. Note that we begin by using only six simulations per bin because the design standards for wind turbines [1,11] suggest that this small number of simulations is permitted for purposes of loads extrapolation. Later, we investigate how short-term load distributions and long-term load predictions change as the number of simulations is increased, and also discuss whether six simulations is adequate or not for the prediction of accurate long-term loads.

Eq. (4) is based on the assumption that the peaks above the chosen threshold in a bin are independent. If a load non-exceedance probability level, p, is of interest, the corresponding load fractile, l_p, based on the POT distribution, is associated with a non-exceedance probability, $p^{1/n}$, and may be estimated as:

$$l_p = F^{-1}_{L_{POT}|X}\left[p^{1/n}\right]. \tag{5}$$

Note that as the selected threshold level is increased, the expected number of peaks that are retained in a specified duration (which is ten minutes here) decreases, and when this number is unity, the POT method approaches the global maximum method, since then on average, one peak is extracted from each simulation. For typical threshold levels, the expected number of retained peaks is significantly larger than unity and, as a result, $p^{1/n}$ can approach values that are close to unity. As an example, if the expected number of peaks above a chosen threshold is 80, then the non-exceedance fractile level for POT data corresponding to the ten-minute median extreme load is $0.5^{1/80} = 0.99137$. If loads corresponding to this probability level are to be established non-parametrically from simulations, at least $1/(1 - 0.99137)$ or 116 peak values above the chosen threshold must be available for the wind speed and wave height bin representing $\boldsymbol{X}$. For tight confidence intervals on such rare load levels, the number of peaks (and thus simulations) might even need to be an order of magnitude higher. Note that extrapolation may often be required then for two reasons: (1) to estimate rarer fractiles (such as, say, the 80th percentile of the ten-minute extreme load instead of the median) as the minimum number of required data may exceed the amount of POT data available from limited simulations; and (2) to have tight confidence intervals on predicted POT load fractiles. Extrapolation is discussed further when addressing long-term loads in the context of the inverse first-order reliability method.

5.2. Long-term loads

With the inverse first-order reliability method, long-term loads may be estimated by using simulations to establish the full conditional distribution for the turbine load variable given wind speed and wave height and then turning the integral equation of

Table 2
Comparison of 20-year loads for blade and tower loads estimated by different methods, when load extremes data are based on the peak-over-threshold method.

Method	20-year load for OoPBM			20-year load for TBM		
	V (m/s)	H_s (m)	OoPBM (MN m)	V (m/s)	H_s (m)	TBM (MN m)
2-D Environmental Contour	12.0	6.2	12.8	12.0	6.2	105.2
2-D Environmental Contour with corrections	12.0	6.2	13.2	12.0	6.2	107.9
3-D Inverse First-Order Reliability Method	14.0	5.5	13.6	16.0	5.5	119.9

Eq. (1) into a search for the maximum load on a locus of points in a 3-D space (representing, V, Hs, and L) associated with the target probability of load exceedance. A reduced effort, though less exact, is possible with the environmental contour method where the 3-D locus searched is reduced to a 2-D one and, additionally, only the conditional median value of L (rather than the full distribution) given V and H_s must be estimated for points on the locus.

We first estimate long-term loads using the 2-D formulation, also referred to as the environmental contour method. Then, we compare 2-D long-term loads with those obtained from a full 3-D inverse reliability approach. We start by using six ten-minute turbine response simulations for each environmental state to establish turbine load statistics, and subsequently investigate the effect of number of simulations on long-term load predictions. All the long-term loads discussed hereinafter correspond to a return period of 20 years, which, according to the wind turbine design standards [1,11], is the target service life for which wind turbines are typically designed.

To derive long-term loads at the site of interest, we require information on the joint distribution of the environmental random variables. For the IEC Class I-B wind regime (for which our turbine model is being considered), we assume that the ten-minute mean wind speed, V, at hub height has an average value of 10 m/s and that it can be described by a Rayleigh distribution. We choose to truncate this distribution below the cut-in wind speed of 4 m/s and above the cut-out wind speed of 24 m/s, since we are interested only in studying turbine loads during operation. The significant wave height, H_s, conditional on the mean wind speed, is assumed to be represented by a two-parameter Weibull distribution. The expected value of H_s given V is based upon the JONSWAP correlation between wind and waves [16], while a coefficient of variation for H_s given V is assumed to be constant at 0.2.

5.2.1. *The 2-D environmental contour (EC) method*

In the 2-D formulation with the EC method, we first establish the environmental contour associated with the desired target probability, using the joint probability density function of mean wind speed and significant wave height, and based on the procedures outlined earlier in the section entitled, "Load Extrapolation Methods". We then seek the maximum value (on this contour) of the median turbine load given $\boldsymbol{X}$. The median load is obtained from POT data by setting p to be 0.5 in Eq. (5). The estimated 20-year loads are presented in Table 2. The 20-year OoPBM load is 12.8 MN m which is associated with a mean wind speed of 12 m/s and a significant wave height of 6.2 m. The 20-year TBM load is 105.2 MN m and it also results from the same wind speed and wave height. That the "design" wind speed is close to the rated wind speed is expected as median extreme turbine loads are largest there, as was discussed earlier. The design wave height of 6.2 m is the larger of the two possible wave heights on the 20-year environmental contour that accompanies the mean wind speed of 12 m/s.

The accuracy of the derived long-term loads by the EC method may be evaluated by determining whether the desired fractile for the POT load requires extrapolation, given the number of peaks above the threshold retained from six simulations. Table 3 shows that for both blade and tower loads, the required POT (non-exceedance) fractiles are smaller than the largest available

Table 3
Required fractiles for the design environmental states with the 2-D environmental contour method.

Load	Average number of peaks, n	Required fractile, $0.5^{1/n}$	Largest empirical fractile
OoPBM	87.2	0.9921	0.9981
TBM	80.2	0.9914	0.9979

empirical fractile, $1 - 1/(6n + 1)$. This suggests that extrapolation is not necessary to arrive at turbine 20-year loads with the EC method; nevertheless, the method has accuracy limitations both because it does not employ the full distribution of turbine loads conditional on $\boldsymbol{X}$ and because even the non-extrapolated fractile is subject to statistical uncertainty due to limited data. To assess both these sources of inaccuracy, we estimate long-term loads using direct integration. We model the conditional load distribution in Eq. (1) as a step function that attains a unit value at the median load. To yield the desired probability level, the 20-year loads are found to be 12.7 MN m and 110.2 MN m, respectively, for OoPBM and TBM, which are very close to those obtained from the environmental contour method. Hence, we conclude that the EC method is not grossly inaccurate relative to an exact integration approach that works with the same data. Still, there are other reasons why the EC-based long-term loads might not be correct; these reasons have to do with incomplete modeling of the conditional distribution of turbine loads given wind speed and wave height. This is addressed next.

5.2.2. *Correction to the EC long-term loads*

While the full distribution of loads (given environmental conditions) can be employed in a 3-D inverse FORM approach, this requires far greater computational effort. An alternative strategy is to apply a correction to the 2-D EC loads [18], as has been successfully demonstrated for onshore turbine long-term loads [4]. In this approach, the neglected response variability in the EC method is attributed to (1) background variability in the median extreme response, $\hat{L}$, which accounts for the variability in the median response with changing environmental states (corresponding to different return periods); and (2) response variability which arises due to different stochastic components for a specific environmental condition (this variability is modeled by quantifying different load fractiles at the same environmental condition). To quantify this overall variability in response, a localized lognormal model is assumed; then, the corrected short-term extreme response, L, may be expressed as $L = \hat{L}\varepsilon$, where ε is taken to be a unit-median random variable that represents the variability in the extreme response for a given set of environmental conditions. Standard deviations of the natural logarithms of these two random variables, $\hat{L}$, and ε, are given by

$$\sigma_{\ln \hat{L}} = \frac{\ln\left(\hat{L}_{T_1}/\hat{L}_{T_2}\right)}{\beta_{T_1} - \beta_{T_2}}; \qquad \sigma_{\ln \varepsilon} = \frac{\ln\left(\varepsilon_{p_2}/\varepsilon_{p_1}\right)}{\Phi^{-1}(p_2) - \Phi^{-1}(p_1)} \tag{6}$$

where T_1 is the target return period (20 years) while T_2 is a slightly shorter return period (taken to be 16 years here), and β_{T1} and β_{T2} are associated reliability indices. Also, with the EC method, p_1 is the median fractile level (i.e., $p_1 = 0.5$) while p_2 is taken to be

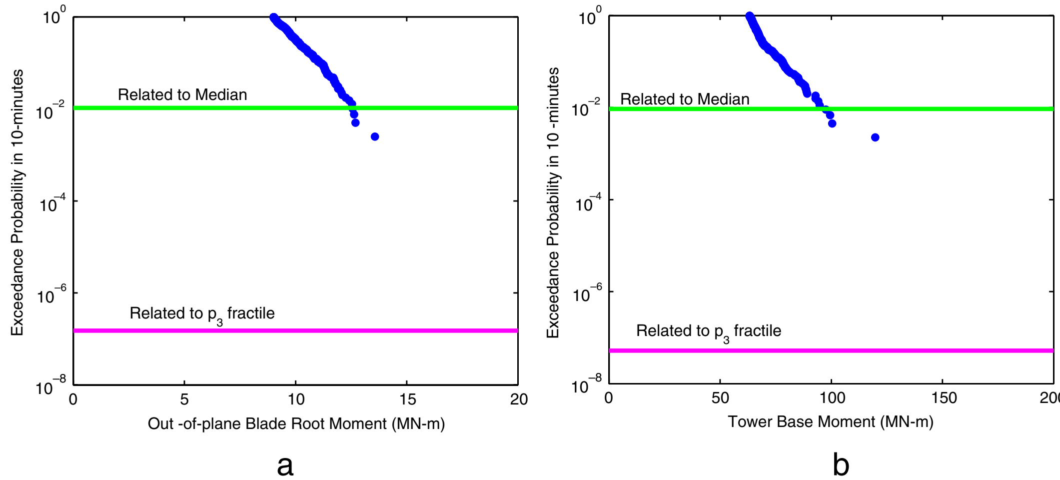

Fig. 7. Load distributions of the POT data for governing environmental states based on 6 simulations for (a) a mean wind speed of 14 m/s and significant wave height of 5.5 m for OoPBM; and (b) a mean wind speed of 16 m/s and a significant wave height of 5.5 m for TBM.

a somewhat higher fractile (here, we take $p_2 = 6/7 = 0.86$), and ε_{p1} and ε_{p2} are associated fractiles. The local lognormal model that is assumed for $\hat{L}$ and ε is best defined by using environmental conditions associated with shorter return periods than T_1 (i.e., $T_1 < T_2$) but with rarer conditional load fractiles than median levels (i.e., $p_2 > p_1 = 0.5$). The correction factor, R, is finally expressed as

$$R = \frac{L_T}{\hat{L}_T} = \exp\left[\left(\sigma_{\ln L} - \sigma_{\ln \hat{L}}\right)\beta_T\right] \tag{7}$$

where $\sigma^2_{\ln L} = \sigma^2_{\ln \hat{L}} + \sigma^2_{\ln \varepsilon}$.

After applying this correction, 20-year loads are estimated to be 13.2 MN m and 107.9 MN m for OoPBM and TBM, respectively (see Table 2). Response variability is largely responsible for the change in the 20-year loads here. However, these corrected blade and tower 20-year loads are only about 3% larger than the 2-D EC values.

5.2.3. 3-D inverse FORM

If instead of only seeking the median extreme load given $\boldsymbol{X}$, the full probability distribution of the turbine extreme load, L, is established by simulations, a search is needed for the maximum value of a different fractile, p_3, on load extremes consistent with each environmental state (V, H_s) and with the specified target probability of failure, P_T (or associated reliability index, β). The desired load fractile level, p_3, equals $\Phi(u_3)$ (see Eq. (3)), and by expressing the standard normal random variables, u_1 and u_2, in terms of the physical environmental random variables using the Rosenblatt transformation [14], we obtain the following expression for p_3:

$$p_3 = \Phi\left[\beta^2 - \left(\Phi^{-1}\left(F_V(v)\right)\right)^2 - \left(\Phi^{-1}\left(F_{H|V}(h)\right)\right)^2\right]^{\frac{1}{2}} \tag{8}$$

where $\Phi()$ and $\Phi^{-1}()$ refer to the standard normal cumulative and inverse cumulative distribution functions, respectively, while $F_V(v)$ and $F_{H|V}(h)$ refer to the cumulative distribution functions for wind speed and for significant wave height (given wind speed), respectively. For POT data, the load fractiles are estimated according to Eq. (5). Note that with the EC method, effectively, p_3 is the conditional median of the load extreme given V and H_s (i.e., $u_3 = 0$ and $p_3 = 0.5$).

With this 3-D inverse FORM approach, the 20-year loads (here obtained by searching only on gridded V–H_s pairs where simulations were carried out) are 13.6 MN m and 119.9 MN m for the blade and tower loads, respectively (see Table 2). These same loads are obtained using the direct integration method, which establishes the accuracy of the 3-D inverse FORM results. These 3-D 20-year loads are roughly 6% and 14% larger, respectively, for the blade and tower loads than those obtained with the 2-D method. Interestingly, the controlling wind speed with the 3-D formulation, which is 14 m/s for the 20-year blade load and 16 m/s for the 20-year tower load, is no longer near the rated wind speed, as was the case with the 2-D formulation. This implies that the full conditional load variability (as a function of wind speed and wave height) is important.

Note that for a pitch-controlled turbine, the rated wind speed is expected to be the wind speed that directly influences long-term extreme loads. Furthermore, in order to reduce the simulation effort, a limited number of wind speeds (as few as three), near rated, may be selected for simulations, as is also suggested in Annex G of the draft IEC guidelines for offshore wind turbines [1]. If we used this criterion, with a small wind speed bin size of 1 m/s, we might miss the controlling-wind speed of 16 m/s that was found here. Ignoring load variability may lead to misleading long-term loads.

We should note that the 2-D EC 20-year loads and the 3-D inverse FORM 20-year loads were calculated based on simulations for a discrete set of gridded values of V and H_s. In subsequent discussions, we examine the environmental state (i.e., V and H_s values) at the 3-D "design" point in Table 2. For the blade and tower loads, these environmental states corresponding, respectively, to $V = 14$m/s, $H_s = 5.5$ m and $V = 16$ m/s, $H_s = 5.5$ m in the 3-D approach, are studied in greater detail in the following.

In order to assess the accuracy of estimated p_3-fractile loads for the design environmental state in this 3-D inverse FORM approach, it is useful to first determine if the required fractile needed to be extrapolated from the POT data. Table 4 shows that, for both loads, the required POT fractiles are significantly higher than the largest available empirical fractile. In our non-parametric model for load distributions, we assume saturation of the tail and somewhat simplistically estimate the required fractile as the largest observed value. The load distribution (Fig. 7), however, shows that the assumption of saturation of tails cannot be justified. As a result, 3-D inverse FORM long-term loads based on this non-parametric approach would clearly be low and unconservative. Next, by performing additional simulations, we seek to obtain more accurate long-term load estimates by establishing short-term loads distributions with more stable tails, at the design environmental states.

Table 4
Required fractiles for the design environmental states with the 3-D inverse FORM approach.

Load	Required load fractile, p_3	Average no. of peaks, n	Required fractile for POT, $p_3^{1/n}$	Largest empirical fractile
OoPBM	0.99998997	66.2	0.99999985	0.9975
TBM	0.99999613	74.2	0.99999995	0.9978

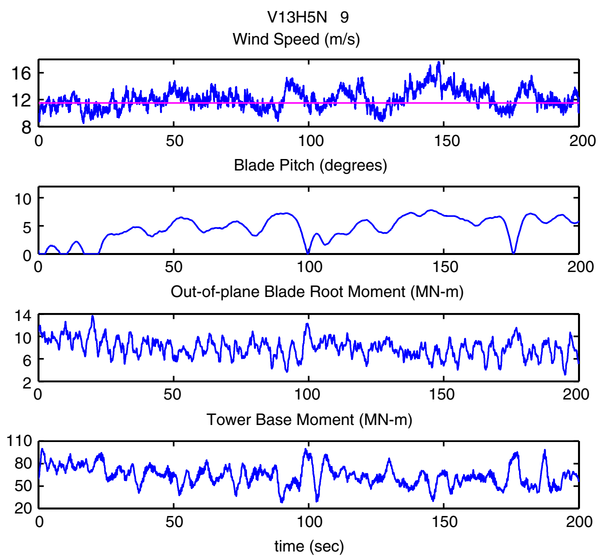

Fig. 8. Time series of wind speed, blade pitch, OoPBM, and TBM for a mean wind speed of 14 m/s and significant wave heights of 5.5 m.

5.2.4. Control actions and number of simulations

An interesting aspect that may be seen from Fig. 7 is that the maximum observed load value, which determines the required extrapolated fractile, is significantly larger than other load values in the tail of the distribution for both OoPBM and TBM. To investigate what conditions bring about this large load, we study in Fig. 8 relevant time histories of wind speed, OoPBM, and TBM along with that of blade pitch angle for a single ten-minute simulation (out of six for the controlling V–H_s combination) that included this large load. The maximum loads were seen to occur when the blade pitch angle suddenly reduced to zero at time instants corresponding roughly to 20 s, 100 s, and 175 s. This is due to the control system for this pitch-controlled turbine, which is such that the blades start to pitch when the instantaneous wind speed exceeds the rated wind speed of 11.5 m/s. At instants when the wind speed falls below the rated speed, the pitch angle reduces to zero and, if the wind speed increases before the blade can pitch back, large loads result.

Since these large loads due to control actions are observed in only one out of six simulations, the distribution tails may only saturate and have better definition than in Fig. 7 if more such large load values result upon performing more simulations. We therefore carry out more simulations for the governing environmental states and find that at least 60 and 150 simulations, respectively, are needed for the blade and tower loads. The corresponding distributions, shown in Fig. 9, also illustrate how the distribution tails fill in and, hence, become more reliable. Clearly, due to blade pitch-control actions, performing only six simulations per environmental state may be inadequate to obtain reliable distributions by means of parametric model fits to the data; this is why non-parametric fractiles were employed with the 2-D and 3-D approaches that were based on only six simulations.

With the more reliable POT load distribution tails made possible due to the larger number of simulations, we attempt fits with parametric models. With a two-parameter Weibull distribution fit to the tails and a least squares basis, Figs. 10(a) and 11(a) show that for the required fractiles of Table 4, 20-year loads of 15.3 MN m and 147.1 MN m result for the blade and tower loads, respectively. These loads are about 13% and 23% larger for blade and tower loads, respectively, than those from the non-parametric approach and based on only six simulations. This is expected since the non-parametric approach unconservatively assumed saturation of distribution tails. As seen, a large number of simulations is required to yield reliable distribution tails and accurate long-term loads. Note that the accuracy of turbine response simulations and, hence, of load distributions and predicted long-term loads also depends on model uncertainties associated with the aeroelastic model and other assumptions made in the stochastic simulation. A limitation of the present study is that we do not address such model uncertainties that are associated with limitations in simulation capability.

6. Comparison of POT and global maxima

In the preceding discussions, we used the peak-over-threshold (POT) data to extract load extremes. An alternative approach is to use global (or epochal) maxima in which only statistics of the single largest load value from each simulation are used. It is of interest to examine how long-term load predictions differ from the two methods. We fit two-parameter Weibull distributions to the tails of global maxima data for the design environmental states, and estimate load fractiles required with the 3-D inverse FORM approach. Figs. 10(b) and 11(b) show these fits for the blade and tower loads, respectively. Long-term load predictions obtained using the global maxima method are 14.5 MN m and 136.6 MN m for the blade and tower loads, respectively; these are only about 5% and 7% smaller for blade and tower loads, respectively, than those obtained using the POT method with parametric distribution fits (Figs. 10(a) and 11(a)). The slightly larger differences in predictions for the tower loads are likely due to relatively poor distribution fits with both methods.

Finally, an important issue when using the POT method is related to the selection of an appropriate threshold level. As the threshold level is increased, the number of peaks decreases and, at an appropriately high threshold, the POT method may result in the same number of load extremes, on average, as the global maxima method. We now estimate required fractiles for the governing environmental state with the 3-D inverse FORM approach using different thresholds and two-parameter Weibull fits for POT distribution tails. Table 5 shows computed fractiles for blade and tower loads. For blade loads, it can be seen that the variation in load fractiles with different thresholds is not significant. The reason is that very good parametric fits, such as those shown in Fig. 10(a), are obtained for all threshold levels. For tower loads, the required load fractiles show slightly greater variation with different threshold choices which may be partly due to less evident and stable trends in distribution tails for these loads (as seen, for example, in Fig. 11(a)). Based on these observations, we conclude that the agreement between long-term loads using the POT and global maxima methods is generally good and is independent of threshold choice as long as distribution tails are reliable enough to allow a good parametric fit.

7. Conclusions

Our objective in this study was to derive long-term loads for a utility-scale 5MW offshore wind turbine sited in 20 m of water. The focus was on the out-of-plane blade bending moment at a blade root and the fore-aft tower base moment at the mudline. Load extremes data needed to establish short-term load distributions

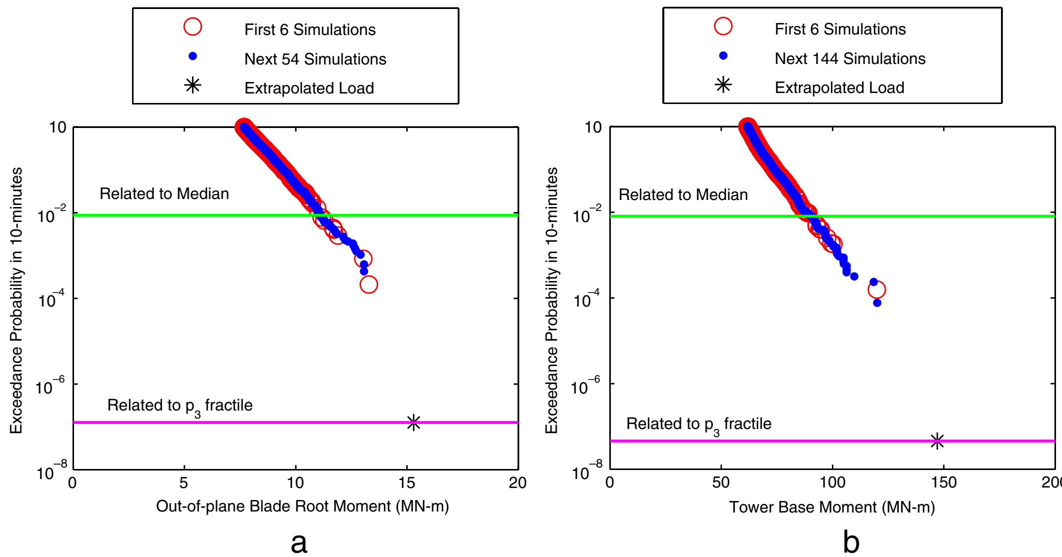

Fig. 9. Load distributions of the POT data for governing environmental states based on (a) 60 simulations of OoPBM for a mean wind speed of 14 m/s and a significant wave height of 5.5 m; and (b) 150 simulations of TBM for a mean wind speed of 16 m/s and a significant wave height of 5.5 m. Extrapolated loads depicted here are estimated from Weibull fits shown in Figs. 10(a) and 11(a).

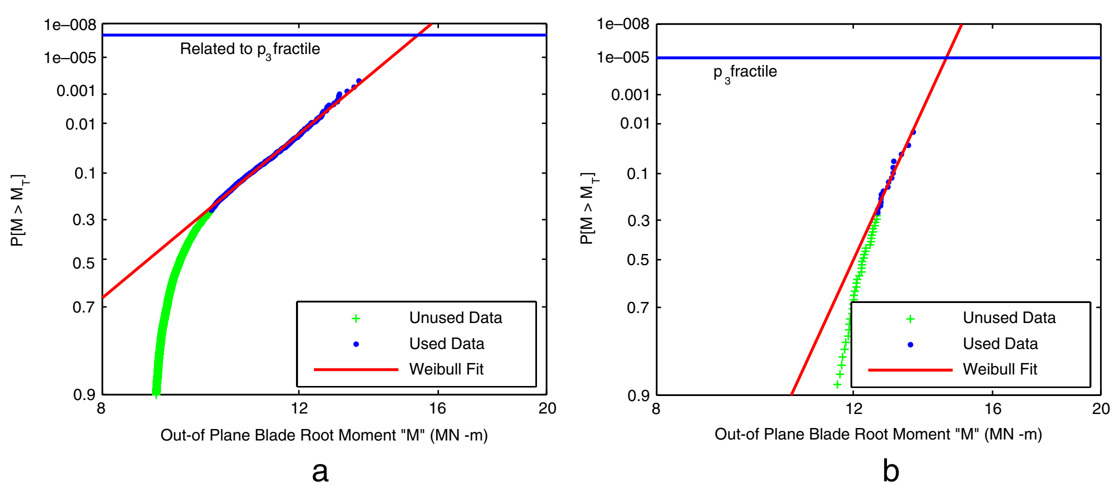

Fig. 10. Two-parameter Weibull distribution fits (a) to POT data, and (b) to global maxima data based on 60 simulations with a mean wind speed of 14 m/s and a significant wave height of 5.5 m for out-of-plane blade moment.

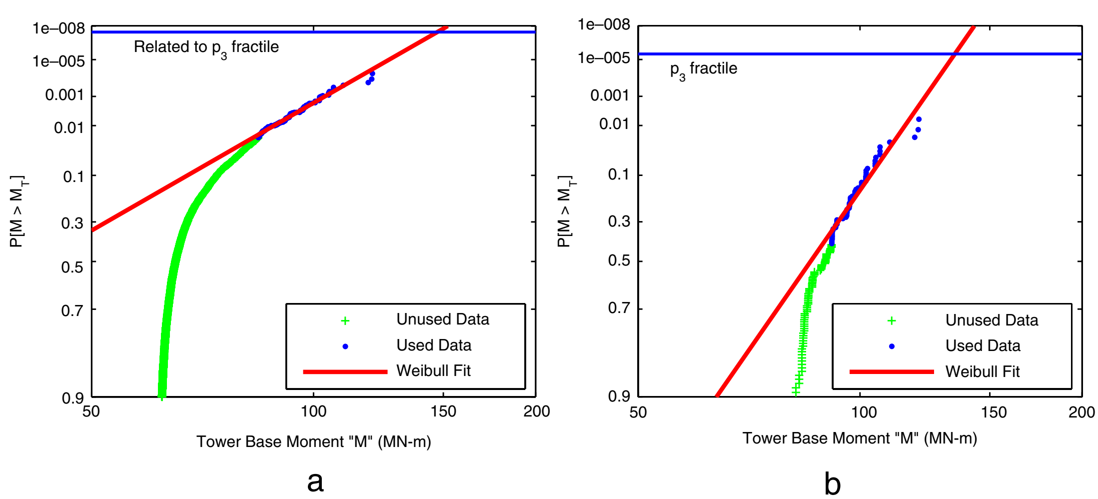

Fig. 11. Two-parameter Weibull distribution fits (a) to POT data, and (b) to global maxima data based on 150 simulations with a mean wind speed of 16 m/s and a significant wave height of 5.5 m for fore-aft tower base moment.

Table 5
Effect of threshold level on the estimate of load fractile for the 20-year environmental state for OoPBM ($p_3 = 0.99998997$) and TBM ($p_3 = 0.99999613$). Threshold = Mean + N_σ × (Standard deviation).

Threshold Level, N_σ	OoPBM ($V = 14$ m/s, $H_s = 5.5$ m)			TBM ($V = 16$ m/s, $H_s = 5.5$ m)		
	Ave. no. of peaks, n	Required exceedance probability, $1 - p_3^{1/n}$	Load fractile (MN m)	Ave. no. of peaks, n	Required exceedance probability, $1 - p_3^{1/n}$	Load fractile (MN m)
1.4	66.8	1.50×10^{-7}	15.3	85.6	4.52×10^{-8}	147.1
1.7	44.7	2.24×10^{-7}	14.9	56.4	6.86×10^{-8}	148.1
2.0	28.9	3.47×10^{-7}	14.8	34.9	1.11×10^{-7}	145.9
2.3	17.1	5.86×10^{-7}	14.7	20.2	1.91×10^{-7}	143.0
2.7	8.1	1.23×10^{-6}	14.6	9.7	3.97×10^{-7}	139.7
3.0	4.0	2.51×10^{-6}	14.6	4.9	7.97×10^{-7}	142.4
Max	1.0	1.00×10^{-5}	14.5	1.0	3.87×10^{-6}	136.6

were extracted from time series of turbine response simulations using the peak-over-threshold method. Long-term loads were estimated using 2-D and 3-D inverse first-order reliability method approaches (the former is also referred to as the environmental contour or EC method) and compared with direct integration. The following are general conclusions for the offshore wind turbine studied:

- The EC method is efficient compared to direct integration but long-term load predictions are based on limited consideration for turbine response variability and can be inaccurate and unconservative.
- The variability in turbine loads for a given environmental state is found to be significant. Due to this, long-term loads based on median values (2-D EC method) of loads given mean wind speed and significant wave height are smaller than those based on higher-than-median fractiles (3-D inverse FORM). The 3-D inverse FORM approach is found to be as accurate as the direct integration approach and is far more efficient; it is recommended for practical wind turbine design applications.
- Importantly, when load variability is considered, the controlling wind speed that influences long-term (20-year) loads is not the rated wind speed (as is often the case) but is somewhat higher than the rated speed.
- A chief source of load variability results from blade-pitch control actions that result in large loads such that the tails of the short-term load distribution are not reliable unless a large number of simulations are performed.

While the above results are based on the peak-over-threshold (POT) method, a comparison of predictions based on the global maxima and POT methods showed that derived long-term loads from both methods were close as long as distribution tails are reliable and well defined.

These conclusions, while particular to the turbine model studied, are useful to consider for any simulation-based exercise that seeks to predict long-term loads for extreme (ultimate) limit states. This study also suggests that the effect of control actions on extreme loads needs careful consideration; in particular it is of interest to investigate methods to account for load variability that arises due to control actions since such variability can alter the tails of load distributions in different ways than loads that result from uncontrolled turbine states.

Acknowledgments

The authors gratefully acknowledge the financial support provided by two grants from the National Science Foundation—CMMI-0449128 (CAREER) and CMMI-0727989. They also acknowledge assistance from Dr. Jason Jonkman at the National Renewable Energy Laboratory with the wind turbine simulation model used in this study.

References

[1] IEC 61400-3. Wind turbines—Part 3: Design requirements for offshore wind turbines. Intl. Electrotechnical Commission, TC88 WG3 Committee Draft; 2005.
[2] Moriarty PJ, Holley WE, Butterfield SP. Extrapolation of extreme and fatigue loads using probabilistic methods. Golden (CO): National Renewable Energy Laboratory; 2004. NREL/TP-500-34421.
[3] Saranyasoontorn K, Manuel L. Design loads for wind turbines using the environmental contour method. J Solar Energy Eng, Trans ASME 2006;128(4):554–61.
[4] Ragan P, Manuel L. Statistical extrapolation methods for estimating wind turbine extreme loads. In: Proc. ASME wind energy symposium. 2007.
[5] Cheng PW. A reliability based design methodology for extreme response of offshore wind turbines. Ph.D. dissertation. The Netherlands: Delft Univ. of Technology; 2002.
[6] Norton E. Investigation into IEC offshore draft standard design load case 1.1. In: Recommendations for design of offshore wind turbines. Denmark: RisøNational Laboratory; 2004.
[7] Saranyasoontorn K, Manuel L. On assessing the accuracy of offshore wind turbine reliability-based design loads from the environmental contour method. Int J Offshore Polar Engrg 2005;15(2):132–40.
[8] Tarp-Johansen NJ. Extrapolation including wave loads—Replacing the distribution of H_s by a suitable percentile. In: Recommendations for design of offshore wind turbines. Denmark: RisøNational Laboratory; 2005.
[9] Sharma JN, Dean RG. Second-order directional seas and associated wave forces. Soc Petroleum Eng J 1981;4:129–40.
[10] Jonkman JM, Buhl Jr ML. FAST user's guide. Golden (CO): National Renewable Energy Laboratory; 2005. NREL/EL-500-38230.
[11] IEC 61400-1. Wind turbines—Part 1: Design requirements. Intl. Electrotechnical Commission, Ed. 3; 2005.
[12] Jonkman BJ, Buhl Jr ML. TurbSim user's guide. Golden (CO): National Renewable Energy Laboratory; 2007. NREL/TP-500-41136.
[13] Winterstein SR, Ude TC, Cornell CA, Bjerager P, Haver S. Environmental contours for extreme response: Inverse FORM with omission factors. In: Proceedings, ICOSSAR-93. 1993.
[14] Rosenblatt M. The spectrum of horizontal gustiness near the ground in high winds. Quart J Roy Meteor Soc 1952;23:470–2.
[15] Jonkman JM, Butterfield S, Musial W, Scott G. Definition of a 5-MW reference wind turbine for offshore system development. Golden (CO): National Renewable Energy Laboratory; 2007. NREL/TP-500-38060.
[16] Chakrabarti SK. Hydrodynamics of offshore structures. UK: WIT Press; 1987.
[17] Madsen HO, Krenk S, Lind NC. Methods of structural safety. Englewood Cliffs (NJ): Prentice Hall; 1986.
[18] Winterstein SR, Engebretsen K. Reliability-based prediction of design loads and responses for floating ocean structures. In: International conference on offshore mechanics and arctic engineering. 1998.